2014

Degradation of the remanent ferromagnetic state under the action of ferroelectric relaxation processes in Co/(1-x)PMN-xPT/Co hybrids: Possible implications on cryogenic and room-temperature applications

Dimosthenis Stamopoulos
Demokritos National Centre For Scientific Research

M Zeibekis
Demokritos National Centre For Scientific Research

G Vertsioti
Demokritos National Centre For Scientific Research

Shujun Zhang
Pennsylvania State University, shujun@uow.edu.au

Degradation of the remanent ferromagnetic state under the action of ferroelectric relaxation processes in Co/(1-x)PMN-xPT/Co hybrids: Possible implications on cryogenic and room-temperature applications

Abstract

Low-dimensional hybrid structures of heterogeneous constituents usually exhibit abnormal properties, a fact that makes such hybrids attractive for various cryogenic and room-temperature applications. Here, we studied $Co/(1 - x)Pb(Mg_{1/3}Nb_{2/3})O_3 -xPbTiO_3 /Co$ (Co/PMN-xPT/Co) with x=0.29 and 0.30, specifically focusing on the evolution of the remanent ferromagnetic state, m_{rem} of the Co outer layers in the whole temperature range from 300K down to 10K, upon application of an external electric field, E_{ex}. We observed that m_{rem} was vulnerable to degradation through the occurrence of electric field-induced magnetic instabilities (EMIs) that appeared only when $E_{ex} \neq 0kV/cm$ and were facilitated as E_{ex} increases. However, EMIs completely ceased below a characteristic temperature $T_{ces} =170K$ even for the maximum $|E_{ex}|=5kV/cm$ applied in this work. A direct comparison of the magnetization data of the Co/PMN-xPT/Co hybrids reported here with the electromechanical properties of the parent PMN-xPT crystals plausibly indicates that EMIs are motivated by the coupling of the ferromagnetic domains of the Co outer layers with the ferroelectric domains of the PMN-xPT crystal. These results highlight the drawback of EMIs in relevant hybrids and delimit the temperature regime for the reliable operation of the Co/PMN-xPT/Co ones studied here.

Disciplines
Engineering | Physical Sciences and Mathematics

Degradation of the remanent ferromagnetic state under the action of ferroelectric relaxation processes in Co/(1-x)PMN-xPT/Co hybrids: Possible implications on cryogenic and room-temperature applications

D. Stamopoulos, M. Zeibekis, G. Vertsioti, and S. J. Zhang

Degradation of the remanent ferromagnetic state under the action of ferroelectric relaxation processes in Co/(1−x)PMN-xPT/Co hybrids: Possible implications on cryogenic and room-temperature applications

D. Stamopoulos,[1,2,a)] M. Zeibekis,[1] G. Vertsioti,[1] and S. J. Zhang[3]
[1]*Institute of Nanoscience and Nanotechnology, National Center for Scientific Research 'Demokritos,',*
Aghia Paraskevi, Athens 153 10, Greece
[2]*Department of Solid State Physics, National and Kapodistrian University of Athens,*
Zografou Panepistimioupolis, 157 84 Zografou, Greece
[3]*Materials Research Institute, The Pennsylvania State University, University Park, Pennsylvania 16801, USA*

Low-dimensional hybrid structures of heterogeneous constituents usually exhibit abnormal properties, a fact that makes such hybrids attractive for various cryogenic and room-temperature applications. Here, we studied Co/$(1 − x)$Pb$(Mg_{1/3}Nb_{2/3})O_3$-xPbTiO$_3$/Co (Co/PMN-xPT/Co) with $x = 0.29$ and 0.30, specifically focusing on the evolution of the remanent ferromagnetic state, m_{rem} of the Co outer layers in the whole temperature range from 300 K down to 10 K, upon application of an external electric field, E_{ex}. We observed that m_{rem} was vulnerable to degradation through the occurrence of electric field-induced magnetic instabilities (EMIs) that appeared only when $E_{ex} \neq 0$ kV/cm and were facilitated as E_{ex} increases. However, EMIs completely ceased below a characteristic temperature $T_{ces} = 170$ K even for the maximum $|E_{ex}| = 5$ kV/cm applied in this work. A direct comparison of the magnetization data of the Co/PMN-xPT/Co hybrids reported here with the electromechanical properties of the parent PMN-xPT crystals plausibly indicates that EMIs are motivated by the coupling of the ferromagnetic domains of the Co outer layers with the ferroelectric domains of the PMN-xPT crystal. These results highlight the drawback of EMIs in relevant hybrids and delimit the temperature regime for the reliable operation of the Co/PMN-xPT/Co ones studied here. © *2014 AIP Publishing LLC*. [http://dx.doi.org/10.1063/1.4893957]

I. INTRODUCTION

Nowadays, low-dimensional hybrid structures are intensively studied due to the abnormal properties that they exhibit. Thus, except for basic research such structures are attractive for the realization of practical devices such as sensitive pressure/acceleration/strain sensors, memory units for the storage of information, energy harvesting, etc.[1–7] A common basis of such hybrids is that they constitute of building blocks that are dimensionally restricted at least in one of the three dimensions and spatially separated since they are in contact only over an interface. A relatively simple, however, interesting class of hybrids that was intensively studied during the last few years had planar topology and was composed of ferromagnetic (FM) films deposited onto a piezoelectric (PE) substrate.[8–15] Intense studies of such so-called magnetoelectric hybrids have been focused on novel applications such as memory devices for electric-write–magnetic-read information storage and magnetic/electric field sensors of increased sensitivity.[16–21] The magnetoelectric effect, direct and inverse, is based on the modulation of electric polarization by a magnetic field and of magnetic polarization by an electric field, respectively, and is a promising candidate mechanism for the realization of devices that can exhibit unique performance through non-volatile processes that require only modest energy consumption. In principle,

magnetoelectric activity can be achieved in two different pathways. Directly, through the coupling of the ferromagnetic and ferroelectric order parameters at the interface and indirectly by using the strain as a mediator, while it stems from the ferroelectric layer it penetrates inside the adjacent ferromagnetic one.[16–21]

Notably, many candidate applications of planar FM/PE hybrids are actually based on the manipulation of the remanent ferromagnetic state, m_{rem} by an external electric field, E_{ex}. For instance, the logical bits "0" and "1" can be physically represented by an m_{rem} oriented along two predetermined opposite directions (let us say +z and –z for out-of-plane m_{rem} orientation). In magnetoelectric memory devices, reversal of m_{rem}, that is bit write, is achieved by using an E_{ex}, thus minimizing energy consumption and prohibiting thermal runaway. This concept is schematically presented in Figure 1(a), where the bottom electrode is a normal metal (NM). Though of importance, the stability of m_{rem} under the presence of an E_{ex} has not been investigated extensively until now.

Here, we study this issue in hybrids that constitute of PE and FM materials, namely the relaxor ferroelectric $(1 − x)$Pb$(Mg_{1/3}Nb_{2/3})O_3$-xPbTiO$_3$ (PMN-xPT) with $x = 0.29$ and 0.30 and Cobalt (Co). The PMN-xPT constituent is in single crystal form, while Co comes in thin film, altogether composing an FM/PE/FM hybrid, as schematically shown in Figures 1(b) and 1(c). In this elemental hybrid unit, the Co outer layers are employed as electrodes to apply an external voltage, V_{ex} (that is an external electric field, E_{ex}) to the PMN-xPT crystal. The strain induced by the PMN-xPT is

a)Author to whom correspondence should be addressed. Electronic addresses: densta@ims.demokritos.gr and densta@phys.uoa.gr
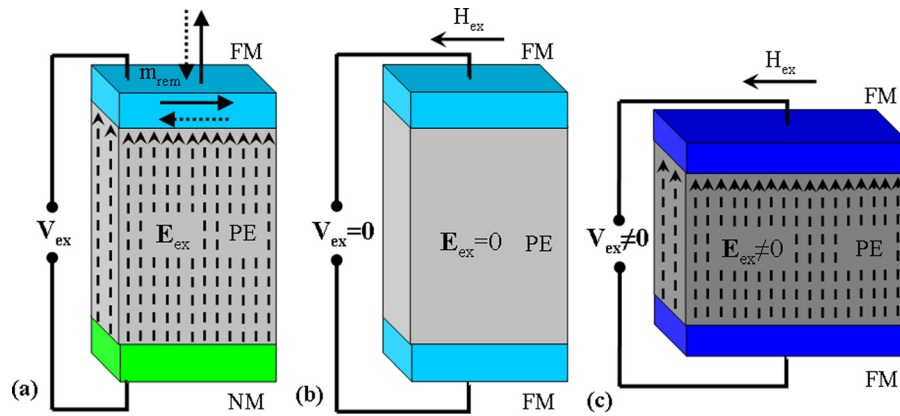
FIG. 1. (a) Schematic presentation of a FM/PE hybrid in which the orientation of the remanent magnetization state, m_{rem} (whether in-plane or out-of-plane) can be controlled by an external electric field, E_{ex} (NM at the bottom electrode designates normal metal). (b) and (c) The FM/PE/FM hybrids studied in this work in (b) the unstrained state with $E_{ex} = 0$ and (c) the strained state with $E_{ex} \neq 0$. In illustrations (b) and (c), the PE interlayer contracts along the direction of E_{ex} application and expands along the transverse ones. The external magnetic field, H_{ex} was always applied parallel to the hybrid surface (in-plane).

ultimately delivered to the Co electrodes, thus modulating their magnetic properties.[15]

Here, we investigate the evolution of the remanent ferromagnetic state, m_{rem} of the Co outer layers in the whole temperature range from 300 K down to 10 K, upon application of an external electric field, E_{ex}. A specially employed measurement protocol reveals that m_{rem} is vulnerable to degradation through the appearance of electric field-induced magnetic instabilities (EMIs) that appear only when $E_{ex} \neq 0$ kV/cm and are facilitated as E_{ex} increases. However, EMIs completely ceased below a characteristic temperature $T_{ces} = 170$ K even for the maximum $|E_{ex}| = 5$ kV/cm applied. By recalling experimental data on the electromechanical properties of the parent PMN-xPT crystals, we propose that the EMIs observed in our Co/PMN-xPT/Co hybrids are possibly motivated by the coupling of the ferromagnetic domains of the Co outer layers with the ferroelectric domains of the PMN-xPT crystal. The possible appearance of EMIs should be investigated in all FM/PE hybrids to test the reliable operation of relevant cryogenic and room-temperature devices.

II. MATERIALS AND METHODS

A. PMN-PT single crystals

The relaxor ferroelectric PMN-xPT crystals with x = 0.29 and 0.30 employed in this work have been grown by a modified Bridgman method using powders of Pb_3O_4, $MgNb_2O_6$, and TiO_2 (purity higher than 99.99%) as starting materials. Details on the preparation process can be found in Refs. 2–4. After growth, the crystals were cut at rectangular shape with dimensions $5 \times 6 \times 0.5$ mm³, with large face perpendicular to [011] direction and side faces of (100) and (0–11). Thus, upon electric field application, the displacements along out-of-plane (that is thickness) and in-plane (that is surface) are based on the values of d_{33}, d_{31}, and d_{32}, being on the order of $+800$, $+500$, and -1200 pC/N (pm/V), respectively. The specific PMN-xPT crystals used here have a rhombohedral to tetragonal phase transition approximately at $T_{RT} = 368$ K and a Curie temperature approximately at $T_C = 408$ K.[2–4]

The as prepared PMN-xPT crystals exhibit a relatively rough surface landscape with a mean surface roughness in the range of 400–600 nm. To ensure a relatively uniform coverage of the crystal surface with the Co thin film (thickness 30–50 nm), we reduced the surface roughness by thorough polishing using fine sandpaper (silicon-carbide P2500). Accordingly, the mean surface roughness was reduced below 100 nm, exhibiting typical values in the range of 30–100 nm.[15]

B. Co thin films

The Co outer layers were RF-sputtered (30 W) using an Edwards 306A unit [Edwards, Sanborn, NY, USA] at 3×10^{-3} Torr of Ar (99.999%) only when a base pressure in the range of 10^{-6}–10^{-7} Torr was established upon adequate pumping. The high-quality FM Co outer layers act as electrodes for the application of the external voltage, V_{ex} (external electric field, E_{ex}) to the PE crystal, so that the produced strain is eventually experienced by the Co thin films, as well. The thickness of Co layers investigated here range within 30 and 50 nm. In this range, the Co layers are quite thick to ensure the uniform coverage of the surface of the *polished* PMN-xPT crystals (thus, enabling application of a uniform E_{ex}), though being thin enough to be entirely susceptible to the strain induced by the adjacent PMN-xPT crystal.

C. Magnetization data

Detailed magnetization measurements were performed by using a homemade, hollow sample rod (outer diameter 3 mm, wall thickness 0.25 mm) hosting two copper wires (diameter 0.1 mm) used to apply the external voltage to the hybrid sample Co/PMN-xPT/Co. We stress that the copper wires were adequately thin to minimize heat transfer from the top part of the sample rod (being outside the cryostat, at room temperature) to the cryostat chamber. This detail is very important to be able to maintain temperatures as low as 10 K and explore the properties of the PE/FM hybrids. A commercial SQUID magnetometer MPMS 5.5 T [Quantum Design, San Diego, CA, USA] was used as the host cryostat for the experiments. The external magnetic field, H_{ex} was applied parallel to the hybrid surface (in-plane). Thus, in

this scheme E_{ex} and H_{ex} were normal to each other (see Figure 1(c)).

The measurement protocol of the isothermal $m(H_{ex})$ loops as function of H_{ex} is as follows: we start from $T = 300\,K$ with zero external magnetic field H_{ex}, apply the external electric field E_{ex}, and cool the hybrid to the desired temperature (electric-field cooled process). Then, H_{ex} is gradually varied from positive to negative saturation while measuring the $m(H_{ex})$ loop. The whole temperature range from $300\,K$ down to $10\,K$ was investigated.

The measurement protocol of the isofield ($H_{ex} = 0$) remanent ferromagnetic state, $m_{rem}(T)$ as function of temperature is as follows: at $T = 300\,K$, while recording $m(H_{ex})$ we increase H_{ex} until positive saturation is reached and then we decrease it to $H_{ex} = 0\,Oe$. This is the remanent ferromagnetic state, m_{rem}. Then, we apply the desired external electric field E_{ex} and decrease the temperature from $T = 300\,K$ down to $T = 10\,K$ while recording $m_{rem}(T)$.

III. RESULTS AND DISCUSSION

Figures 2(a) and 2(b) show representative $m(H_{ex})$ loops obtained at $T = 10\,K$ and $T = 300\,K$, respectively, for a Co(30 nm)/PMN-0.30PT/Co(30 nm) hybrid subjected to various external electric field, E_{ex} values. Detailed sets of similar data obtained in the whole temperature range from $T = 10\,K$ to $T = 300\,K$ clearly documented that the modulation of the coercive field, H_c of the outer Co electrodes upon application of E_{ex} occurr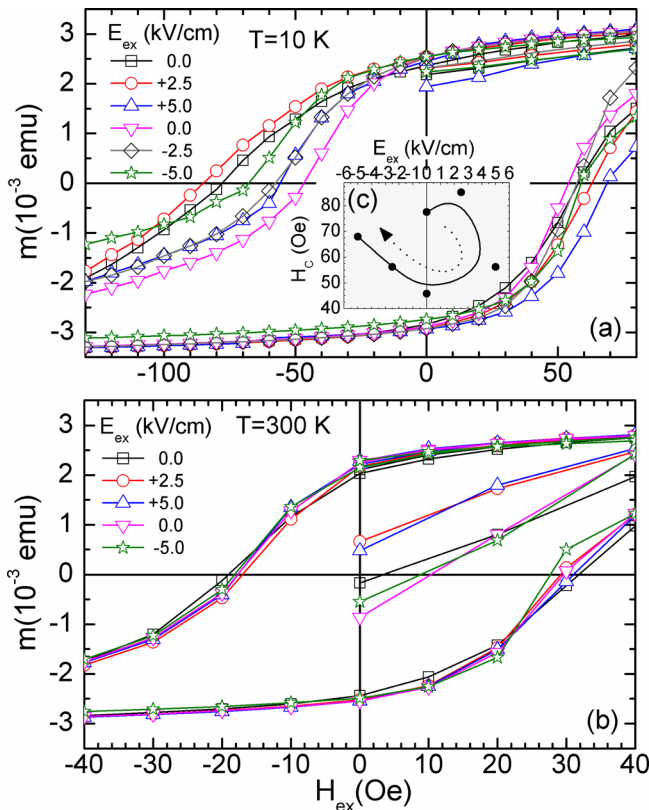ed only for temperatures $T < 150\,K$. This verifies the results already presented in Ref. 15 for Co(30 nm)/PMN-0.29PT/Co(30 nm) hybrids. Quantitatively, as shown in inset (c) for $T = 10\,K$, the coercive field, H_c of the decreasing branch exhibits a noticeable percentage modulation, as defined from equation $[(H_c^{max} - H_c^{min})/H_c^{min}]100\%$, being on the order of 153% between $E_{ex} = 2.5\,kV/cm$ and $E_{ex} = 0\,kV/cm$.

The possible mechanisms that motivate and/or facilitate the modulation of the coercive field, H_c upon application of E_{ex} have been discussed in Ref. 15. In this work, we focused on the investigations of the stability of the remanent ferromagnetic state, m_{rem} of the Co outer layers upon application of E_{ex} to the PMN-0.30PT single crystal. The whole temperature range from $T = 300\,K$ down to $T = 10\,K$ was investigated. To this effect, after preparation of state m_{rem} at $T = 300\,K$, we applied the desired external electric field, E_{ex} and recorded how $m_{rem}(T)$ evolves upon decrease of temperature down to $T = 10\,K$. Figure 3 shows a representative case of how m_{rem} was prepared at $T = 300\,K$. Then, E_{ex} was applied and $m_{rem}(T)$ was recorded as temperature was decreased.

Typical results are shown in Figures 4(a), 4(b), and 4(c) for $E_{ex} = 0\,kV/cm$, $E_{ex} = \pm 2.5\,kV/cm$, and $E_{ex} = \pm 5.0\,kV/cm$, respectively. These data clearly document the occurrence of abrupt changes of the recorded $m_{rem}(T)$ in the form of distinct suppression events ($m_{rem}(T)$ degradation) that we term magnetic instabilities (MIs). MIs exist in other areas of magnetism (i.e., Barkhausen effect; see Refs. 22–26) and superconductivity (i.e., flux-lines avalanche effect; see Refs. 27–32). However, in those cases, the MIs have different origin. Regarding the Barkhausen effect,[22] MIs mainly occur during reversal of the magnetization and associate with a sequence of distinct jumps accompanied by crackling noise. This is due to the interaction between magnetic domains and magnetic domain walls with quench and thermal disorder. By quench disorder we mean structural disorder, whether of point (e.g., atomic vacancies) or correlated (e.g., dislocations) nature, while by thermal disorder we mean the thermal energy. The competition between quench and thermal disorder can result in nucleation/reversal of magnetic domains and depinning of magnetic domain walls that subsequently are free to

FIG. 2. Isothermal $m(H_{ex})$ loops for a Co(30 nm)/PMN-0.30PT/Co(30 nm) hybrid for various E_{ex} values at (a) $T = 10\,K$ and (b) $T = 300\,K$ focused in both cases in the low-field regime. Inset (c) of panel (a) presents the modulation of the coercive field, H_c of the decreasing branch, upon variation of E_{ex}.
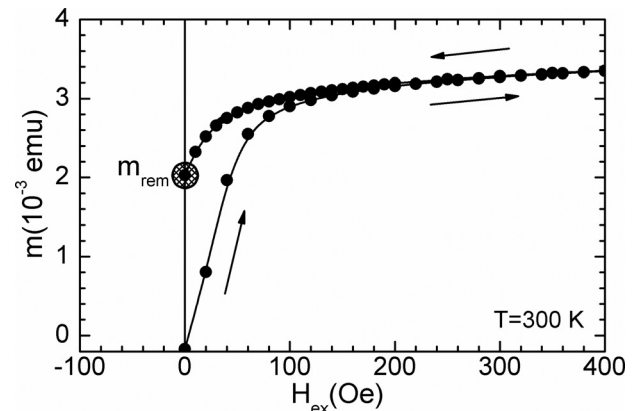

FIG. 3. Presentation of how the remanent ferromagnetic state, m_{rem} of a Co(30 nm)/PMN-0.30PT/Co(30 nm) hybrid is prepared after increase of the external magnetic field, H_{ex} until positive saturation and subsequent decrease to zero. State m_{rem} is prepared at $T = 300\,K$ before application of the external electric field, E_{ex}.
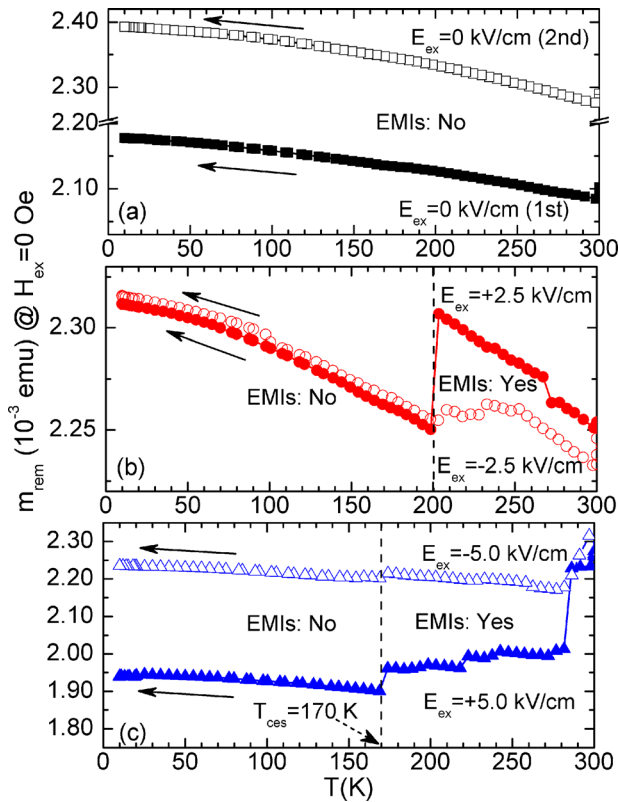
FIG. 4. Evolution of the remanent ferromagnetic state, $m_{rem}(T)$ for a Co(30 nm)/PMN-0.30PT/Co(30 nm) hybrid upon temperature decrease from $T = 300\,K$ down to $T = 10\,K$ for (a) $E_{ex} = 0\,kV/cm$, (b) $E_{ex} = \pm 2.5\,kV/cm$, and (c) $E_{ex} = \pm 5.0\,kV/cm$. In (b) and (c), EMIs are observed in the high temperature regime delimited by the vertical/dashed lines. In (c), T_{ces} denotes the cessation temperature below which EMIs do not exist.

move.[23–26] Obviously, from a technological point of view the Barkhausen effect is important since it is detrimental to the stability of magnetic data storage devices. Referring to the flux-lines avalanche effect,[27] it is associated with the interplay of three energy scales, the interaction energy between flux lines, the pinning energy of flux lines with quench disorder, and finally the thermal disorder.[27–32] It is well known that during the entrance of flux lines in a superconductor they self-assemble in a critical state[33,34] so that the current reaches a critical value, at the cutting edge just before movement of flux lines takes place. An avalanche event is observed when thermal activation motivates overcritical conditions and drives abrupt movement of bundles of flux lines that ultimately appears in the form of magnetization jumps.[27–32]

As we show here, Figures 4(a)–4(c), in our case the observed MIs were exclusively motivated by the externally applied electric field, E_{ex} thus we coin the term electric field-induced MIs (EMIs). Specifically, from Figure 4(a) it is evident that EMIs do not exist for $E_{ex} = 0\,kV/cm$ since only a gradual increase of $m_{rem}(T)$ was observed upon decreasing the temperature. On the contrary, from Figures 4(b) and 4(c), it is fairly documented that when $E_{ex} \neq 0\,kV/cm$ EMIs emerged. Most important, EMIs are facilitated as E_{ex} increases since, first the temperature range where EMIs occur gets wider and second the overall degradation of $m_{rem}(T)$ increases. Quantitatively, at $E_{ex} = +2.5\,kV/cm$ (Figure 4(b)), we observe an intense EMI that produces a

$m_{rem}(T = 200\,K)$ percentage degradation of order 2.5%, while at $E_{ex} = +5.0\,kV/cm$ (Figure 4(c)) the cumulative action of many EMIs produces a much higher $m_{rem}(170\,K < T < 300\,K)$ percentage degradation on the order of 16.4%. Notably, even in the case of the maximum $|E_{ex}| = 5\,kV/cm$ applied in this work, EMIs were not observed below 170 K. The appearance of EMIs only at high temperatures and the complete cessation below $T_{ces} = 170\,K$ imply the interplay of thermal activation and pinning processes. However, from the data of Figures 4(a)–4(c), it is obvious that thermal energy alone is not adequate to overcome energy barriers that delimit metastable states of m_{rem} and thus to motivate MIs in the absence of E_{ex}.

Recent publications[35–37] have focused on the experimental exploration of the properties of PMN-xPT crystals in the whole temperature range from room temperature down to cryogenic conditions. Those works[35–37] evidenced that all important characteristics (relative dielectric constant K, elastic compliance coefficient s_{ij}, piezoelectric coefficients d_{ij}, etc.) exhibit a bimodal behaviour between the high and low temperature regimes with an inflection regime, $T_{inf} \approx 170\,K$.[37] For instance, this is clearly illustrated in Figure 5 below, where the temperature evolution of the piezoelectric coefficient d_{31} is shown for a PMN-xPT crystal with $x = 0.33$. We clearly see that, as temperature decreases from $T = 300\,K$, the piezoelectric coefficient $d_{31}(T)$ exhibits a power-law–like decrease that ends at $T_{inf} \approx 170\,K$. Below $T_{inf} \approx 170\,K$, $d_{31}(T)$ starts to decrease again following a second power-law–like behavior.

A direct comparison of the $m_{rem}(T)$ data of Figures 4(a)–4(c), obtained on a Co(30 nm)/PMN-xPT/Co(30 nm) hybrid with $x = 0.30$, with the $d_{31}(T)$ curve of Figure 5, obtained on a PMN-xPT crystal with similar composition of $x = 0.33$, show strong evidence that $T_{ces} \approx T_{inf}$. Thus, we can plausibly assume that there is a direct correlation of the underlying mechanisms responsible for the cessation of EMIs (Figures 4(a)–4(c)) and the decrease of d_{31} (Figure 5)

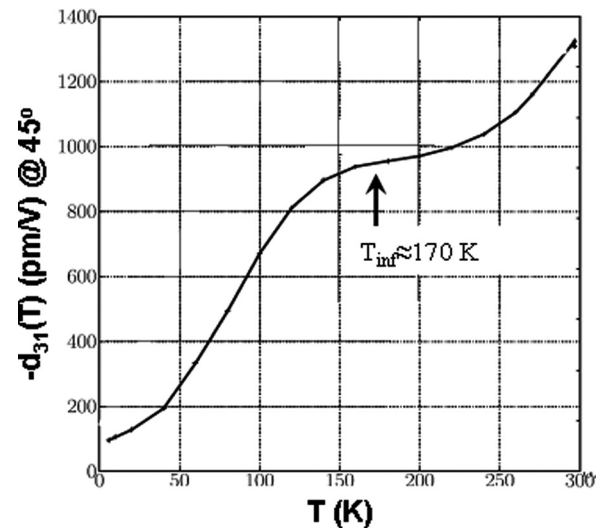FIG. 5. Temperature evolution of the transverse strain coefficient d_{31} for a PMN-xPT crystal with $x = 0.33$. Reprinted with permission from Martin *et al.*, J. Appl. Phys. **111**, 104108 (2012). Copyright 2012 American Institute of Physics.

as temperature decreases below T_{ces} and T_{inf}, respectively. In Refs. 35–37, the decrease of d_{31} and the formation of a plateau below T_{inf} (Figure 5) were ascribed to the establishment of intense collective pinning of ferroelectric (macro)-domain walls by structural disorder (i.e., point defects)[38] that prohibits their motion. It is natural then to assume that in the Co(30 nm)/PMN-xPT/Co(30 nm) hybrids studied here there is a coupling between ferroelectric domains of the PMN-xPT crystal and ferromagnetic domains of the Co outer layers so that the latter are forced to follow the dynamics of the former. Under this point of view, instabilities of ferromagnetic domains (that is EMIs) are observed in the high temperature regime since they are motivated by the reconfiguration of ferroelectric domains (e.g., via partial rotation and/or motion), while EMIs cease below T_{ces} since ferroelectric domains are relatively quenched below T_{inf} once collective pinning by structural disorder dominates over thermal activation so that not only the complete reversal but also the partial rotation and/or motion is prohibited.

This aforementioned coupling between ferromagnetic and ferroelectric domains/polarization rotations can be phenomenologically assumed to be indirect that is mediated by strain, as observed in other magnetoelectric layered hybrids studied in the literature.[20,21] This is indirectly supported by the correlation observed between the strain coefficient and the magnitude of m_{rem} degradation. Quantitatively, the m_{rem} degradation observed in Figures 4(b) and 4(c) reads 2.5% for $E_{ex} = +2.5$ kV/cm and 16.4% for $E_{ex} = +5.0$ kV/cm, respectively. For the same PMN-xPT crystals, at room temperature, the respective in-plane (that is along the surface) strain reads $S \approx 0.03\%$ for $E_{ex} = +2.5$ kV/cm and $S \approx 0.06\%$ for $E_{ex} = +5.0$ kV/cm (data not shown) as measured directly from the Strain-Electric field curve (for instance, see Figure 6 of Ref. 39 for PMN-xPT with x = 0.27 and 0.31). Thus, we see that the increased strain correlates with increased m_{rem} degradation.

The cessation of EMIs at $T < T_{ces} = 170$ K observed here correlates nicely with the experimental fact, originally reported in Ref. 15 and confirmed here, that the modulation of both coercive field, H_c and saturation magnetization, m_{sat} by the external electric field, E_{ex} is practically effective only below a characteristic temperature, T_{ch} that is at $T < T_{ch} = 150$ K. A representative case is shown in Figure 6 for a Co(30 nm)/PMN-0.29PT/Co(30 nm) hybrid and for a

maximum electric field, $E_{ex} = 6$ kV/cm very close to the one, $E_{ex} = 5$ kV/cm applied in the Co(30 nm)/PMN-0.30PT/Co(30 nm) hybrid discussed above, Figures 2–4. Thus, we can justifiably assume that $T_{ces} \approx T_{ch}$. Based on this assumption, we propose that for $T > T_{ces} \approx T_{ch}$ both H_c and m_{sat} effectively become independent of E_{ex} since the measured magnetization relaxes rapidly, through the occurrence of EMIs, to a rather stable state due to thermal activation. On the contrary, for $T < T_{ces} \approx T_{ch}$ both H_c and m_{sat} depend on E_{ex} since the relaxation of magnetization is subjected to slow dynamics once thermal activation gets weak in comparison to pinning processes. This explanation agrees nicely with the arguments reported in Refs. 36 and 37 regarding the different dielectric relaxation processes observed at cryogenic and room-temperature conditions for the parent PMN-xPT crystals.

IV. CONCLUSIONS

In this work, we investigated FM/PE/FM hybrids based on constituent materials that are well studied and easily prepared, namely PMN-xPT single crystal with x = 0.29 and 0.30 and Co thin film. We specifically focused on the evolution of the remanent ferromagnetic state, m_{rem} of the Co outer layers in the whole temperature range from 300 K down to 10 K, upon application of an external electric field, E_{ex}. A specially employed measurement protocol revealed that m_{rem} is vulnerable to degradation through the occurrence of EMIs that appear only when $E_{ex} \neq 0$ kV/cm and are facilitated as E_{ex} increases. However, EMIs completely ceased below a characteristic temperature $T_{ces} = 170$ K even for the maximum $|E_{ex}| = 5$ kV/cm applied in this work. A direct comparison of the magnetization data of the Co/PMN-xPT/Co hybrids reported here with the electromechanical properties of the parent PMN-xPT crystals plausibly indicates that EMIs are motivated by the coupling of the ferromagnetic domains of the Co outer layers with the ferroelectric domains of the PMN-xPT crystal. Since an unstable m_{rem}, that is vulnerable to degradation, stands against utilization in applications, we propose that the appearance of EMIs should be investigated in all FM/PE hybrids that are candidates for realization of relevant devices.
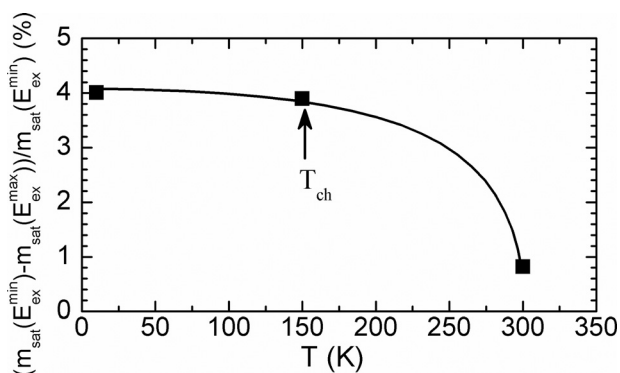
FIG. 6. Temperature evolution of the modulation degree of the saturation magnetization, m_{sat} for a Co(30 nm)/PMN-0.29PT/Co(30 nm) hybrid between $E_{ex}^{min} = 0$ KV/cm and $E_{ex}^{max} = 6$ KV/cm.

[1]S. Zhang and F. Li, J. Appl. Phys. **111**, 031301 (2012).
[2]F. Li, S. Zhang, Z. Xu, X. Wei, J. Luo, and T. R. Shrout, J. Appl. Phys. **108**, 034106 (2010).
[3]X. B. Li and H. S. Luo, J. Am. Ceram. Soc. **93**, 2915 (2010).
[4]S. J. Zhang, S. M. Lee, D. H. Kim, H. Y. Lee, and T. R. Shrout, J. Am. Ceram. Soc. **91**, 683 (2008).
[5]K. Uchino, *Ferroelectric Devices* (Dekker, New York, 2000).
[6]J. F. Scott, *Ferroelectric Memories* (Springer Verlag, Berlin, 2000).
[7]S. Tadigadapa and K. Mateti, Meas. Sci. Technol. **20**, 092001 (2009).
[8]S. Polisetty, W. Echtenkamp, K. Jones, X. He, S. Sahoo, and Ch. Binek, Phys. Rev. B **82**, 134419 (2010).
[9]S. Brivio, D. Petti, R. Bertacco, and J. C. Cezar, Appl. Phys. Lett. **98**, 092505 (2011).
[10]S. Geprägs, A. Brandlmaier, M. Opel, R. Gross, and S. T. B. Goennenwein, Appl. Phys. Lett. **96**, 142509 (2010).

[11]Z. Huang, I. Stolichnov, A. Bernand-Mantel, J. Borrel, S. Auffret, G. Gaudin, O. Boulle, S. Pizzini, L. Ranno, L. H. Diez, and N. Setter, Appl. Phys. Lett. **103**, 222902 (2013).

[12]T. H. E. Lahtinen, K. J. A. Franke, and S. Dijken, Sci. Rep. **2**, 258 (2012).

[13]Z. X. Cheng, X. L. Wang, S. X. Dou, M. Osada, and H. Kimura, Appl. Phys. Lett. **99**, 092103 (2011).

[14]Q. X. Zhu, M. M. Yang, M. Zheng, W. Wang, Y. Wang, X. M. Li, H. S. Luo, X. G. Li, H. L. W. Chan, and R. K. Zheng, J. Alloys Compd. **581**, 530 (2013).

[15]D. Stamopoulos, M. Zeibekis, and S. J. Zhang, J. Appl. Phys. **114**, 134309 (2013).

[16]W. Eerenstein, N. D. Mathur, and J. F. Scott, Nature **442**, 759 (2006).

[17]W. Eerenstein, M. Wiora, J. L. Prieto, J. F. Scott, and N. D. Mathur, Nature Mater. **6**, 348 (2007).

[18]M. Bibes and A. Barthélémy, Nature Mater. **7**, 425 (2008).

[19]J.-T. Heron, M. Trassin, K. Ashraf, M. Gajek, Q. He, S. Y. Yang, D. E. Nikonov, Y.-H. Chu, S. Salahuddin, and R. Ramesh, Phys. Rev. Lett. **107**, 217202 (2011).

[20]C. Thiele, K. Dörr, O. Bilani, J. Rödel, and L. Schultz, Phys. Rev. B **75**, 054408 (2007).

[21]N. Lei, T. Devolder, G. Agnus, P. Aubert, L. Daniel, J.-V. Kim, W. Zhao, T. Trypiniotis, R. P. Cowburn, C. Chappert, D. Ravelosona, and P. Lecoeur, Nat. Commun. **4**, 1378 (2013).

[22]H. Barkhausen, Z. Phys. **20**, 401 (1919).

[23]A. Benassi and S. Zapperi, Phys. Rev. B **84**, 214441 (2011).

[24]G. Durin and S. Zapperi, *The Science of Hysteresis*, edited by G. Bertotti and I. D. Mayergoyz (Academic, New York, 2006), Vol. II, p. 181.

[25]S. Zapperi, P. Cizeau, G. Durin, and H. E. Stanley, Phys. Rev. B **58**, 6353 (1998).

[26]D.-H. Kim, S.-B. Choe, and S.-C. Shin, Phys. Rev. Lett. **90**, 087203 (2003).

[27]R. G. Mints and A. L. Rakhmanov, Rev. Mod. Phys. **53**, 551 (1981).

[28]P. Esquinazi, A. Setzer, D. Fuchs, Y. Kopelevich, E. Zeldov, and C. Assmann, Phys. Rev. B **60**, 12454 (1999).

[29]P. S. Swartz and C. P. Bean, J. Appl. Phys. **39**, 4991 (1968).

[30]R. G. Mints and E. H. Brandt, Phys. Rev. B **54**, 12421 (1996).

[31]D. Stamopoulos, A. Speliotis, and D. Niarchos, Supercond. Sci. Technol. **17**, 1261 (2004).

[32]D. Stamopoulos and D. Niarchos, Physica C **417**, 69 (2004).

[33]C. P. Bean, Rev. Mod. Phys. **36**, 31 (1964).

[34]A. M. Campbell and J. E. Evetts, Adv. Phys. **21**, 199 (1972).

[35]F. Li, S. Zhang, Z. Xu, X. Wei, J. Luo, and T. Shrout, Appl. Phys. Lett. **96**, 192903 (2010).

[36]F. Wang, W. Shi, S. W. Or, X. Zhao, and H. Luo, Mater. Chem. Phys. **125**, 718 (2011).

[37]F. Martin, H. J. M. ter Brake, L. Lebrun, S. J. Zhang, and T. Shrout, J. Appl. Phys. **111**, 104108 (2012).

[38]Y. N. Huang, X. Li, Y. Ding, Y. N. Wang, H. M. Shen, Z. F. Zhang, C. S. Fang, S. H. Zhou, and P. C. W. Fung, Phys. Rev. B **55**, 16159 (1997).

[39]D. Stamopoulos and S. J. Zhang, J. Alloys Compd. **612**, 34 (2014).